

Reversible surface morphology in shape-memory alloy thin films

M. J. Wu,¹ W. M. Huang,^{1,a)} Y. Q. Fu,² F. Chollet,¹ Y. Y. Hu,¹ and M. Cai³

¹*School of Mechanical and Aerospace Engineering, Nanyang Technological University, 50 Nanyang Avenue, Singapore 639798, Singapore*

²*School of Engineering and Physical Sciences, Heriot Watt University, Edinburgh EH14 4AS, United Kingdom*

³*Department of Engineering Technology, University of Houston, Houston, Texas 77204, USA*

(Received 7 January 2008; accepted 23 December 2008; published online 10 February 2009)

Reversible surface morphology can be used for significantly changing many surface properties such as roughness, friction, reflection, surface tension, etc. However, it is not easy to realize atop metals at micron scale around ambient temperature. In this paper, we demonstrate that TiNi and TiNi based (e.g., TiNiCu) shape-memory thin films, which are sputter-deposited atop a silicon wafer, may have different types of thermally-induced reversible surface morphologies. Apart from the well-known surface relief phenomenon, irregular surface trenches may appear in the fully crystallized thin films, but disappear upon heating. On the other hand, in partially crystallized thin films, the crystalline structures (islands) appear in chrysanthemum-shape at high temperature; while at room temperature, the surface morphology within the islands changes to standard martensite striations. Both phenomena are fully repeatable upon thermal cycling. The mechanisms behind these phenomena are investigated. © 2009 American Institute of Physics. [DOI: 10.1063/1.3075773]

I. INTRODUCTION

The surface morphology of materials can be altered by, for instance, the phase transformation [e.g., surface relief in shape-memory alloys (SMAs) (Ref. 1)] or wrinkling (e.g., heating/cooling of thin metallic films atop elastomeric polymers,^{2,3} and in thermal cycling of oxidized viscous thin films atop elastic substrates^{4,5}). One of the particular interesting points of this phenomenon is that the formed patterns can be at micrometer scale and they are highly in order.⁶⁻¹⁰ Reversible surface morphology can be used for significantly changing many surface properties such as roughness, friction, reflection, surface tension, etc. However, it is not easy to realize atop metals at micron scale around ambient temperature.

It is well known that in bulk SMAs, during the martensitic transformation upon cooling, austenite transforms into twinned martensite and the original flat surface becomes rough (i.e., surface relief) without any macroscopic shape change. In the reverse transformation, the rough surface of martensite changes back to smooth surface (at high temperature austenite state). Hence, surface relief in SMAs is fully reversible. Wrinkles atop polymer substrates disappear only at high temperature at which the thermal strains in the substrate and coating are zero.¹¹ However, in many ceramic and metallic materials, the wrinkles are permanent and even grow with further thermal cycling known as ratcheting.¹⁰

Recently, similar surface relief has also been observed in the sputter-deposited TiNi and TiNiCu shape-memory thin films (e.g., Refs. 12 and 13, Fig. 1). In this paper, we investigate two other types of thermally-induced reversible surface morphologies, namely, surface trench and surface wrinkle in TiNiCu shape-memory thin films.

II. EXPERIMENT

Ti₅₀Ni₄₇Cu₃ shape-memory thin films of about 3.5 μm thick were fabricated by cosputtering of a Ti(55 at. %)Ni(45 at. %) target (3-in. diameter, rf, 400 W) and a pure Cu target (3-in. diameter, dc, 2 W) on standard 4-in. 450 μm thick (100) silicon wafers. Two types of films were prepared with different deposition and annealing temperatures, which are listed in Table I.

The thin films deposited at room temperature (about 25 °C) are amorphous. The ones deposited atop a heated wafer (e.g., at 350 °C) have crystalline structures, which can be confirmed by the x-ray diffraction (XRD) test (Philips PW3719 XRD, Cu-K_α, 40 KV/30 mA). For both as-deposited films, upon thermal cycling, except for a slight variation in surface roughness no apparent change in surface morphology was found, even under a temperature controlled atomic force microscope (AFM, SFT-9800, Shimadzu).¹

Both films were then left in air for a few days before postannealing in a vacuum chamber for 1 h (with parameters shown in Table I). Curvature test was carried out to measure stress in the films upon subsequent thermal cycling¹⁴ and differential scanning calorimeter (DSC) test (TA instrument 2920) was performed on the peel-off films to determine the phase transformation temperatures.

III. RESULTS AND DISCUSSION

A. Thin film deposited at elevated temperature

The films deposited at 350 °C and then annealed at 450 °C are fully crystalline martensite at room temperature, which become austenite upon heating to around 80 °C. Observation using a temperature controlled AFM reveals that at room temperature there are many trenches on the film surface. A typical one is shown in Fig. 2(a). However, all trenches disappear at a high temperature (e.g., 100 °C) as

^{a)}Author to whom correspondence should be addressed. Electronic mail: mwmhuang@ntu.edu.sg.

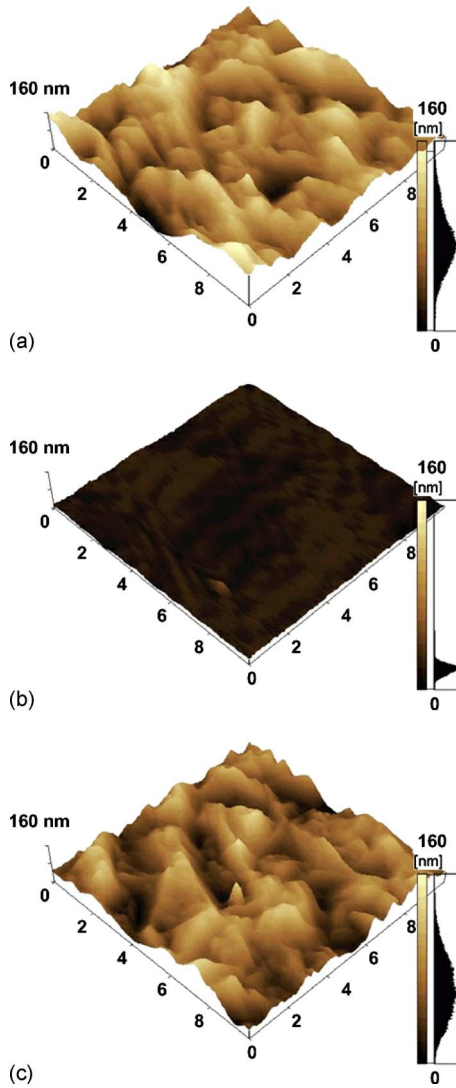


FIG. 1. (Color online) Reversible surface relief morphology in a TiNi SMA thin film in a heating/cooling cycle (deposited at 25 °C, and then annealed at 450 °C) (AFM image, $10 \times 10 \mu\text{m}^2$).

shown in Fig. 2(b). When the sample is cooled back to room temperature, almost identical trenches reoccupy the surface as shown in Fig. 2(c). This phenomenon is repeatable even after many thermal cycles. Further scanning electron microscopy (SEM) observation indicates that these trenches are neither grain boundary nor the surface relief induced by the martensitic transformation (Fig. 3). Figure 4 shows a series of cross-sectional views of a typical trench upon heating, which suggests the occurrence of a kind of elastic buckling at room temperature. This is seemingly similar to thermally induced ratcheting that requires: (1) an elastic thin layer, which is under compression; (2) a relatively soft elastic-

TABLE I. Deposition and annealing conditions for two types of films.

	Trench sample	Chrysanthemum shape sample
Deposition temperature	350 °C	25 °C
Deposition durations	4 h	4 h
Annealing temperature	450 °C	350 °C
Annealing durations	1 h	1 h

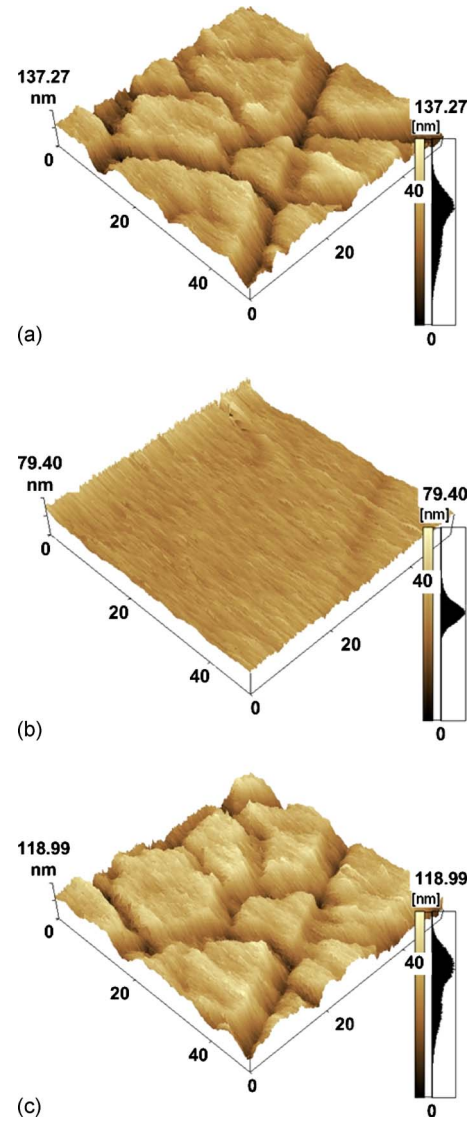


FIG. 2. (Color online) Reversible trenches morphology in a heating/cooling cycle of a TiNiCu thin film deposited at 350 °C, left in air for a few days, and then postannealed at 450 °C (AFM image, $50 \times 50 \mu\text{m}$).

plastic metallic layer underneath the elastic thin layer.¹⁰ It should be pointed out that depending on the softness of the substrate, buckling can happen at a low compressive stress in the elastic thin layer even if the elastic layer is very thin.^{10,11}

It is well known that a thin oxide and oxygen diffusion layer, tens of nanometers thick, can be formed on the surface of TiNi based thin films (e.g., Refs. 15–17), which can be verified from x-ray photoelectron spectroscopy (XPS) analysis. SMA thin films are relatively *soft* at low temperature (associated with martensite) and can consequently serve as the elastic-plastic metallic layer. A large *plastic* strain can easily occur, and most importantly, for SMAs, this *plastic* deformation is fully recoverable upon heating.

To verify the role of TiO_2 in the above-observed phenomenon, we immersed half of a sample into an etching solution (a mixture of 40% nitric acid and 1.5% hydrofluoric acid, and diluted with deionized water) for about 12 s to remove the oxide layer. The sample was then subjected to another thermal cycle and cooled down to room temperature.

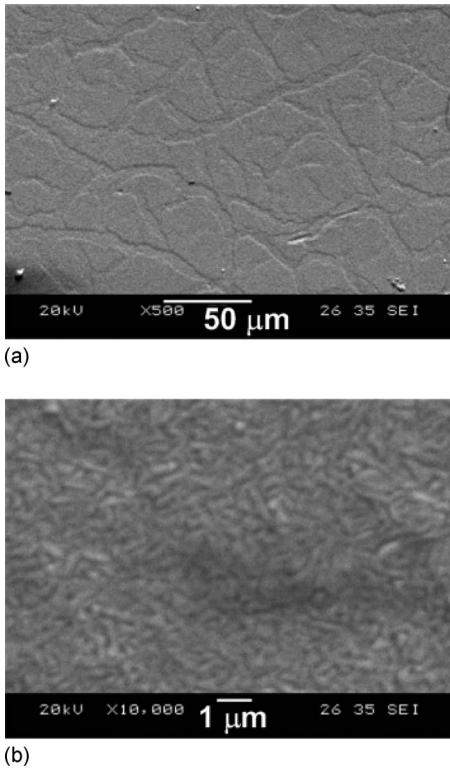


FIG. 3. SEM image (a) and a zoom-in view (b) which reveals that the trenches are not grain boundary.

Except for etching pits, no trenches were observed on the surface of the etched part, while trenches persisted in the part without etching (Fig. 5). This proves that the oxide layer, TiO₂, is indeed a requirement for the trenching phenomenon. Since the as-deposited thin films atop a heated wafer do not show any trench at room temperature (not even after the sample placed in air for a long period), we may further conclude that the subsequent high temperature annealing is another prerequisite for the appearance of the trenches.

As the shape-memory thin film is much thinner than the substrate (4 μm vs 450 μm), the stress and strain in the thin film (σ_f and ϵ_f , respectively) are almost uniform¹⁸ and can be obtained from the measured curvature (K) versus temperature variation (ΔT) relationship through¹⁹

$$\sigma_f = \frac{K \bar{E}_s t_s^3}{6 t_f (t_f + t_s)}, \tag{1}$$

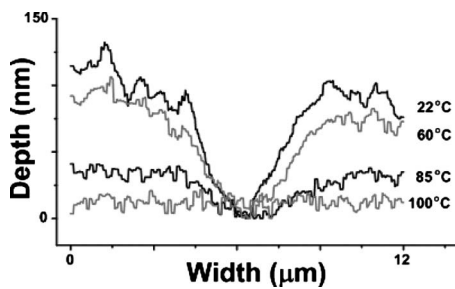


FIG. 4. Cross section of a trench in Ni_{45.2}Ti_{50.3}Cu_{4.5} upon heating from 22 °C to 100 °C.

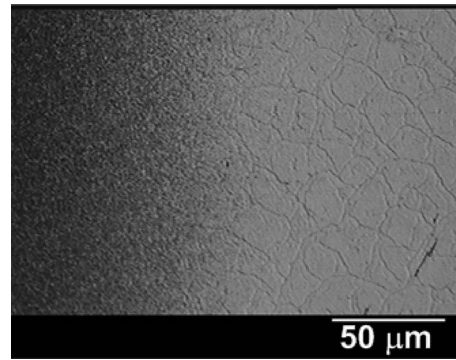


FIG. 5. Comparison of surface at room temperature with etching (left part) and without etching (right part).

$$\epsilon_f = -\frac{1}{6} K \left[4 t_s + t_f \left(5 + \frac{t_f}{t_f + t_s} \right) \right] + \alpha_s \Delta T, \tag{2}$$

where $\bar{E} [=E/(1-\nu)]$ is the biaxial modulus (E is the Young's modulus and ν is the Poisson ratio), α is the coefficient of thermal expansion, and t is the thickness. Here, subscripts s and f denote the substrate (i.e., silicon wafer) and SMA thin film, respectively. The initial temperature should correspond to the equilibrium state, i.e., roughly the subsequent annealing temperature. In the above analysis, the contribution of the oxide layer is neglected, since it is much thinner than other layers.

The total strain in the oxide layer (ϵ_o) can be expressed as (hereinafter, subscript o stands for oxide layer)

$$\epsilon_o = \epsilon_f + \epsilon_{th} + \epsilon_e, \tag{3}$$

where ϵ_{th} , thermal mismatch strain,

$$\epsilon_{th} = (\alpha_o - \alpha_f) \Delta T \tag{4}$$

is due to the difference in the coefficient of thermal expansion between the oxide layer and SMA thin film, and ϵ_e ($=\sigma_o/\bar{E}_o$) is the elastic strain in the oxide layer. Taking the annealing temperature as the initial equilibrium state, using the measured three-dimensional surface data to calculate the strain in TiO₂ and DSC result of SMA thin film for the transformation progress, we can estimate the stress evolution in the SMA thin film and TiO₂ upon thermal cycling as plotted in Fig. 6. The typical material properties for the numerical analysis are listed in Table II. From Fig. 6, it can be con-

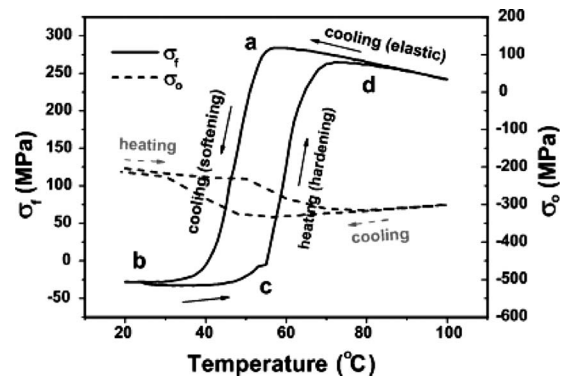


FIG. 6. Evolution of stresses in a thin film (Ni_{45.2}Ti_{50.3}Cu_{4.5}) and TiO₂ upon thermal cycling.

TABLE II. Typical values of some thermomechanical properties of bulk TiO₂ (Ref. 20), TiNi (Ref. 21), and Si (Ref. 22).

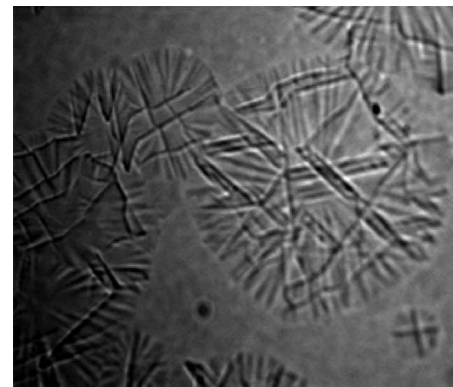
		α (°C ⁻¹)	E (GPa)	ν
TiO ₂		9×10^{-6}	282.76	0.28
TiNi	Austenite	11×10^{-6}	83	0.33
	Martensite	6.6×10^{-6}	20	
Silicon (100)		2.6×10^{-6}	130.2	0.28

firming that after annealing the top TiO₂ layer is always under compression (between -200 to -300 MPa) within the temperature range of thermal cycle. We can then conclude that the reversible trenches in SMA thin films are indeed the result of buckling of TiO₂ due to the large compressive stress.

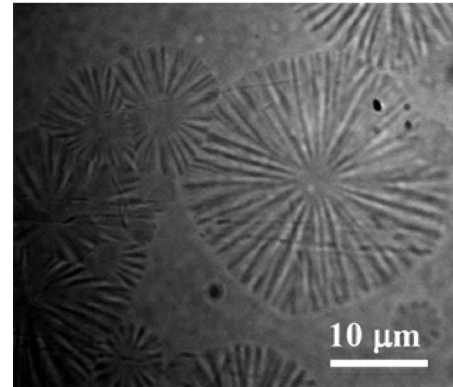
B. Thin film deposited at room temperature

For the TiNiCu films deposited at room temperature and then annealed at 350 °C, optical microscope observation reveals that clusters of circular islands are surrounded by a featureless matrix [Fig. 7(a)]. These islands have a diameter ranging from a few microns to 30 microns. Detailed TEM and XRD analyses confirmed that these circular patterns are single crystals and the matrix is amorphous.²³ These chrysanthemum-shaped patterns are similar to that observed in ratcheting of metallic thin films with a thin elastic oxidation layer on top.¹⁰ Because the annealing temperature (i.e., 350 °C in this study) is in the range of amorphous-to-crystalline transition temperature of the TiNiCu thin films, crystallization can occur by nucleation and growth. Depending on the film chemical composition, annealing temperature and time (and therefore the kinetics), partial crystallization is possible.²⁴ Within the crystalline islands (single crystal within an island as reported in Refs. 23 and 24) that is relatively soft at this temperature as compared with the surrounding hard amorphous material, buckling can occur in the top oxide layer of the islands under a small compressive stress if the size of the islands is large enough.²³ As the islands are austenite single crystals, the buckling pattern should be more or less symmetric, i.e., symmetric circular buckling shape or chrysanthemum shape. This pattern can be well kept upon cooling before martensite occurs. In contrast to the formation of trenches in Fig. 2, the martensitic transformation results in the transition of austenite (high order of symmetry) to much soft martensite (low order of symmetry). As such, surface relief offers a way to partially release the compressive stress in the oxide layer (instead of trenches, due to the constraint from the boundary of islands).

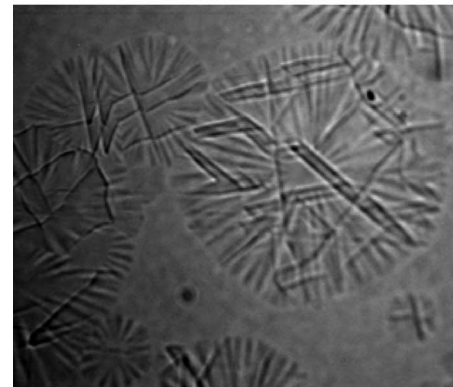
In situ optical microscopy observation reveals that upon heating the interweaving martensitic plate structures [Fig. 7(a)] are gradually replaced by chrysanthemum-shaped pattern [Fig. 7(b)], which does not change upon further heating to above 120 °C. Upon cooling, the reversible transformation in SMAs ensures the formation of the same relief patterns from the chrysanthemum-shaped pattern in the islands.²³ If the martensitic transformation finish temperature is below room temperature, the surface morphology will re-



(a)



(b)



(c)

FIG. 7. Reversible surface morphology in a heating/cooling cycle between relief and chrysanthemum patterns within islands of TiNiCu films deposited at 25 °C. Left in air for a few days and then postannealed at 350 °C (optical microscope image) (Ref. 23).

main as the chrysanthemum-shaped pattern, rather than surface relief morphology.

Our further experimental work also verified that the similar reversible trench and chrysanthemum-shaped patterns can be found on the surface of sputtered and annealed TiNi shape-memory thin films. However, without the deliberate process for oxidation before postannealing at high temperature, no reversible morphology can be obtained as in many previous experiments.

IV. CONCLUSIONS

We reported the surface morphological changes from sputter-deposited TiNi based shape-memory thin films atop

silicon wafers. Mechanisms behind the different types of reversible surface morphologies of the films upon thermal cycling have been identified. In the fully crystallized thin films, trenches may emerge upon cooling and disappear upon heating. While in the partially crystallized ones, surface relief is resolved by the formation of martensite striation upon cooling and chrysanthemum-shaped pattern appears upon heating. We show that the thin oxide layer (TiO_2) on the top surface of shape-memory thin films plays a critical role in forming elastic buckling in SMA thin films upon thermal cycling. Annealing or reannealing after surface oxidation is an important procedure for the phenomenon of reversible trenches. One may utilize these phenomena in thin film SMAs for dramatically altering the surface roughness or morphology within a small temperature fluctuation. Potential applications of this work include developing actuators for MEMS, manufacturing diffractive optical elements for optical and mechanical applications with greater load bearing ability, and better durability.²⁵

ACKNOWLEDGMENTS

This work was partially support by an AcRF (Grant No. RG9/04) from Nanyang Technological University, Singapore and the Key Provincial Laboratory Open Fund of Liaoning Province at Shenyang Jianzhu University (Grant No. JG200710), People's Republic of China. Experimental help from S. Sanjabi and Z. H. Barber from University of Cambridge, U.K. is acknowledged.

¹Q. He, W. M. Huang, M. H. Hong, M. J. Wu, Y. Q. Fu, T. C. Chong, F. Chollet, and H. J. Du, *Smart Mater. Struct.* **13**, 977 (2004).

²N. Bowden, S. Brittain, A. G. Evans, J. W. Hutchinson, and G. M. Whitesides, *Nature (London)* **393**, 146 (1998).

³H.-L. Zhang, T. Okayasu, and D. G. Bucknall, *Eur. Polym. J.* **40**, 981 (2004).

⁴M. Y. He, A. G. Evans, and J. W. Hutchinson, *Acta Mater.* **48**, 2593 (2000).

⁵G. Parry, C. Coupeau, J. Colin, A. Climeiere, and J. Grilhe, *Acta Mater.* **52**, 3959 (2004).

⁶K. Bhattacharya and R. D. James, *Science* **307**, 53 (2005).

⁷J. Liang, R. Huang, H. Yin, J. C. Sturm, K. D. Hobart, and Z. Suo, *Acta Mater.* **50**, 2933 (2002).

⁸P. J. Yoo and H. H. Lee, *Phys. Rev. Lett.* **91**, 154502 (2003).

⁹X. Chen and J. W. Hutchinson, *Scr. Mater.* **50**, 797 (2004).

¹⁰S. H. Im and R. Huang, *Acta Mater.* **52**, 3707 (2004).

¹¹X. Chen and J. W. J. Hutchinson, *ASME Trans. J. Appl. Mech.* **71**, 597 (2005).

¹²Y. Q. Fu, H. J. Du, W. M. Huang, S. Zhang, and M. Hu, *Sens. Actuators, A* **112**, 395 (2004).

¹³Q. He, M. H. Hong, W. M. Huang, T. C. Chong, Y. Q. Fu, and H. J. J. Du, *J. Micromech. Microeng.* **14**, 950 (2004).

¹⁴Y. Y. Hu and W. M. Huang, *J. Appl. Phys.* **96**, 4154 (2004).

¹⁵A. Ishida and M. Sato, *Acta Mater.* **51**, 5571 (2003).

¹⁶Y. Fu, H. Du, S. Zhang, and W. Huang, *Mater. Sci. Eng., A* **403**, 25 (2005).

¹⁷Y. Q. Fu, S. Zhang, M. J. Wu, W. M. Huang, H. J. Du, J. K. Luo, A. J. Flewitt, and W. I. Milne, *Thin Solid Films* **515**, 80 (2006).

¹⁸W. M. Huang, Y. Y. Hu, and L. An, *Appl. Phys. Lett.* **85**, 6173 (2004).

¹⁹W. M. Huang, Y. Y. Hu, and L. An, *Appl. Phys. Lett.* **87**, 201904 (2005).

²⁰J. F. Shackelford and W. Alexander, *CRC Materials Science and Engineering Handbook* (CRC, Cleveland, 2001).

²¹W. M. Huang, *Mater. Des.* **23**, 11 (2002).

²²Y. Okada and Y. Tokumaru, *J. Appl. Phys.* **56**, 314 (1984).

²³Y. Q. Fu, S. Sanjabi, Z. H. Barber, T. W. Clyne, W. M. Huang, M. Cai, J. K. Luo, A. J. Flewitt, and W. I. Milne, *Appl. Phys. Lett.* **89**, 171922 (2006).

²⁴M. Cai, Y. Q. Fu, S. Sanjabi, Z. H. Barber, and J. T. Dickinson, *Surf. Coat. Technol.* **201**, 5843 (2007).

²⁵Y. Zhang, Y. T. Cheng, and D. S. Grummon, *Appl. Phys. Lett.* **89**, 041912 (2006).